

Are “Bondi-Hoyle Wakes” detectable in clusters of galaxies?

Irini Sakelliou

Mullard Space Science Laboratory, University College London, Holmbury St Mary, Dorking, Surrey RH5 6NT, UK

30 October 2018

ABSTRACT

In clusters of galaxies, the reaction of the intracluster medium (ICM) to the motion of the co-existing galaxies in the cluster triggers the formation of unique features, which trace their position and motion. Galactic wakes, for example, are an apparent result of the ICM/galaxy interactions, and they constitute an important tool for deciphering the motion of the cluster galaxies.

In this paper we investigate whether Bondi-Hoyle accretion can create galactic wakes by focusing the ICM behind moving galaxies. The solution of the equations that describe this physical problem provide us with observable quantities along the wake at any time of its lifetime. We also investigate which are the best environmental conditions for the detectability of such structures in the X-ray images of clusters of galaxies.

We find that significant Bondi-Hoyle wakes can only be formed in low temperature clusters, and that they are more pronounced behind slow-moving, relatively massive galaxies. The scale length of these elongated structures is not very large: in the most favourable conditions a Bondi-Hoyle wake in a cluster at the redshift of $z=0.05$ is 12 arcsec long. However, the wake’s X-ray emission is noticeably strong: the X-ray flux can reach ~ 30 times the flux of the surrounding medium. Such features will be easily detectable in *Chandra*’s and *XMM-Newton*’s x-ray images of nearby, relatively poor clusters of galaxies.

Key words: galaxies: clusters: general – galaxies: interaction – intergalactic medium – galaxies: kinematics and dynamics – X-rays: galaxies

1 INTRODUCTION

In clusters of galaxies, the interactions of the intracluster medium (ICM) with a moving cluster galaxy is expected to modify both the local properties of the surrounding medium and the galaxy itself. One of the manifestations of such interactions is the Bondi-Hoyle (B-H) accretion (Bondi & Hoyle 1944). This physical process can be pictured as follows: as the galaxy is moving in the cluster, ICM particles are deflected by the galaxy’s gravity and concentrate behind it, into the galactic wake.

Intuitively, one might think that B-H accretion creates overdense and cool regions of enhanced x-ray emission behind the galaxies. As a consequence, the hot interstellar media (ISM) of these galaxies look as if they have been disfigured: instead of being azimuthally symmetric they appear elongated, or as if they have a ‘plume’ of x-ray emission attached to them. Such elongated features have now been identified in the x-ray images of clusters of galaxies (e.g.,

around NGC 1404 in the Fornax cluster of galaxies; Jones et al. 1997). An up-to-date list of wake candidates can be found in Stevens, Acreman & Ponman (1999).

Bondi-Hoyle accretion is not the only manifestation of the ISM/ICM interactions which creates elongated features behind moving galaxies. Ram pressure stripping can also shape the ISM in such a way that it appears elongated. The difference in the nature of the two elongated structures is apparent: a B-H wake comprises of ICM material, while a ram pressure-induced wake contains galactic material (ISM).

Unfortunately, instrumentation prior to *Chandra* and *XMM-Newton* has not generally allowed the separation of the pure galactic and the wake components, either spatially or spectroscopically. Only the elliptical galaxy M86 has offered us the opportunity to gain more insight into the nature of its wake (Rangarajan 1995). The observational fact that the metallicity of M86’s wake is higher than the metallicity in the surrounding medium, has been used to assign it a galactic origin. It seems most probable that in the case of

M86, stripping of its ISM is currently in action, and that its wake consists mostly of galactic material. No other well studied example is currently known. The danger arising from the inability to separate the wake's emission from the galaxy itself, is that the analysis of the galaxy's X-ray data would lead to false conclusions for the characteristics of its X-ray halo. The dilution of ISM gas by the ICM gas in the B-H wake could, for example, lead to confusing results for the metal abundances in elliptical galaxies.

It should be understood that under certain conditions, B-H accretion and ram pressure stripping may occur simultaneously, creating wakes which contain a mixture of both galactic and intracluster material. Recent numerical simulations by Stevens et al. (1999) have shown that this picture can be indeed correct. However, it is not clear yet which are the effects of each separate process, and how the dominance of one process over the other depends on the environmental parameters. It is expected, though, that dense ICMs and high galactic speeds favour ram pressure stripping. However, the results of the B-H accretion cannot be foreseen so easily. If we want to understand the action of B-H accretion and be able to find the environmental dependences, we have to study this process in its first principles.

The aim of this paper is to disentangle the two physical processes by studying the action and results of the B-H accretion. We address questions such as: under which conditions B-H accretion occurs in clusters of galaxies; which clusters are the best candidates for detecting B-H wakes; and whether x-ray observations with the *Chandra* and *XMM-Newton* observatories can reveal B-H wakes.

The remainder of this paper is organized as follows: in §2 we present the methodology we followed to calculate the properties of B-H wakes, section §3 discusses the constraints and input parameters imposed by the problem itself. The results of the simulations are presented in §4. Finally, in §5 our results are compared to available observations, and simulations of similar physical processes.

2 CREATION AND EVOLUTION OF A B-H WAKE

Consider a test volume behind a moving galaxy. As the galaxy travels in the cluster at the speed of v_{gal} , particles of the ICM are deflected by the galactic gravitational potential, and directed into this volume. The ICM particles that are influenced by the galaxy's attraction, and modify their direction of motion, are the ones contained within a cylinder of radius equal to the accretion radius (R_{acc}):

$$R_{\text{acc}} = \frac{2GM_{\text{gal}}}{v_{\text{gal}}^2 + c_s^2} \quad (1)$$

(Bondi 1952), where M_{gal} and c_s are the mass of the galaxy and the local speed of sound respectively.

In time dt , the particles that enter the wake, at a position x along the accretion axis, are the ICM's particles which were initially in a shell of width db and length $ds = v_{\text{gal}}dt$, and had impact parameter b (see Fig 1):

$$d^2z_{\text{acc}}(x) = 2\pi b v_{\text{gal}} n_{\text{ICM}} db dt, \quad (2)$$

where n_{ICM} is the number density of the surrounding medium.

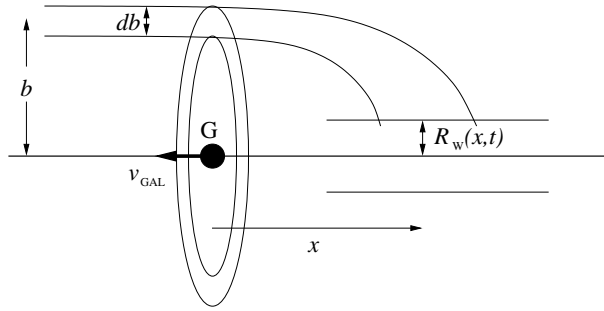


Figure 1. Schematic diagram of the configuration used for the calculations of the B-H accretion. The galaxy 'G' is moving in a cluster of galaxies through an ICM of number density n_{ICM} .

The particles that start with an impact parameter b land in the wake along the accretion axis at a distance x from the galaxy. Assuming that the ballistic approximation is valid (see §3.1.2) we find that the position x is given by:

$$x = \frac{-GM_{\text{gal}} + (G^2 M_{\text{gal}}^2 + v_{\text{gal}}^4 b^2)^{1/2}}{v_{\text{gal}}^2}. \quad (3)$$

The velocity, $v_{\text{in}}(x)$, at the position x on the accretion axis relates to the initial velocity of the ICM's particles (v_{gal}) by:

$$v_{\text{in}}(x) = v_{\text{gal}} \frac{b}{x}. \quad (4)$$

The effect of these incoming ICM's particles is i) the increase of the internal energy [$E_{\text{int}}(x, t)$] of the wake, and ii) its confinement by the pressure [$P_{\text{acc}}(x, t)$]:

$$P_{\text{acc}}(x, t) dx dt = \frac{\mu m_p v'_{\text{in}}(x, t)}{2\pi R_w(x, t)} d^2 z_{\text{acc}}(x), \quad (5)$$

where $d^2 z_{\text{acc}}(x)$ is given by eq. 2, and $R_w(x, t)$ is the radius of the wake at the position x (Fig. 1). In eq. 5, $v'_{\text{in}}(x, t)$ is the velocity of the incoming particles in the wake's frame of reference, and it is given by:

$$v'_{\text{in}}(x, t) = v_{\text{in}}(x) + \frac{dR_w(x, t)}{dt} \quad (6)$$

As the galaxy travels through the ICM, the constant replenishment of the wake with particles and energy causes a continuous change to its properties. The evolution of the wake is governed by two equations:

- the conservation of energy:

$$\begin{aligned} \frac{dE_{\text{int}}(x, t)}{dt} &= \\ &= -L_{\text{bol}}(x, t) - P_w(x, t) \frac{dV_w(x, t)}{dt} + \frac{dE_{\text{incom}}(x, t)}{dt} \end{aligned} \quad (7)$$

- and the conservation of the momentum (p):

$$\frac{dp}{dt} = \int [P_w(x, t) - P_{\text{ICM}} - P_{\text{acc}}(x, t)] d\sigma \quad (8)$$

where σ is the surface containing the wake.

In the above two equations, $P_w(x, t)$, and P_{ICM} are the pressures of the wake and the surrounding ICM respectively. In eq. 7, the first term [$L_{\text{bol}}(x, t)$] represents the energy radiated away via thermal bremsstrahlung, and it is calculated in the appendix A. The second term is the work done by

the wake to the surrounding medium. The third term is the energy added to the wake by the accreted particles :

$$dE_{\text{incom}}(x, t) = \frac{3}{2} d^2 z_{\text{acc}}(x, t) k T_w(x, t), \quad (9)$$

where it was assumed that the incoming particles have enough time to thermalize with the existing particles in the wake, and reach a Maxwellian distribution at the temperature of $k T_w(x, t)$ (see §3).

3 SIMULATIONS

Equations 8 and 7 were solved numerically to predict the temperature [$k T_w(x, t)$], and the number density [$n_w(x, t)$] of the wake at any position x along the accretion axis. The time step of the integration process was constant and such as to allow the gas in the wake to reach a Maxwellian equilibrium. Knowing the temperature and density at any time t , and position x , the luminosity [$L_{\text{bol}}(x, t)$] can be found from equation A1. The central surface brightness along the accretion axis [$\Sigma_{E_1 - E_2}(0)$], and the wake's surface brightness distribution are calculated using eq. A5 and A4 respectively.

The initial conditions for the simulations were chosen to comply with the conditions associated with this problem (Table 1) and are derived in the next sections. The chosen values for the parameters of the ICM and the galaxies' velocity represent the conditions found in poor and moderately rich clusters of galaxies, which as will become apparent in the next sections, are the fertile environments for B-H wake creation.

3.1 Input constraints and initial conditions

3.1.1 The mass of the galaxy

The accretion radius (eq. 1), defines the size of the region around the cluster galaxy in which the galactic gravitational potential is strong enough to change the direction of motion of all the ICM particles which happen to be inside that region, and direct them into the wake. Particles approaching the galaxy with impact parameters less than R_{acc} are deflected into the wake, while particles with $b > R_{\text{acc}}$ continue their motion passed the galaxy unaffected. Therefore, an apparent, and simple condition for a galaxy to have a B-H wake, is that its accretion radius should be larger than its size.

As is obvious from eq. 1, the potential of a wake being formed behind a cluster galaxy depends on the velocity and the mass of the galaxy. If we assume an average velocity for the galaxies in a cluster of $v_{\text{gal}} = \sqrt{3}\sigma$, where the velocity dispersion σ is given by the $\sigma - T$ relation in clusters of galaxies:

$$\sigma \sim 400 \left(\frac{k T_{\text{ICM}}}{\text{keV}} \right)^{0.5}, \text{ (km s}^{-1}\text{)} \quad (10)$$

(White et al. 1997; Wu, Fang & Xu 1998), and a sound speed c_s of:

$$c_s = 516 \left(\frac{k T_{\text{ICM}}}{\text{keV}} \right)^{0.5}, \text{ (km s}^{-1}\text{)} \quad (11)$$

we find that the condition $R_{\text{acc}} \geq R_{\text{gal}}$ gives:

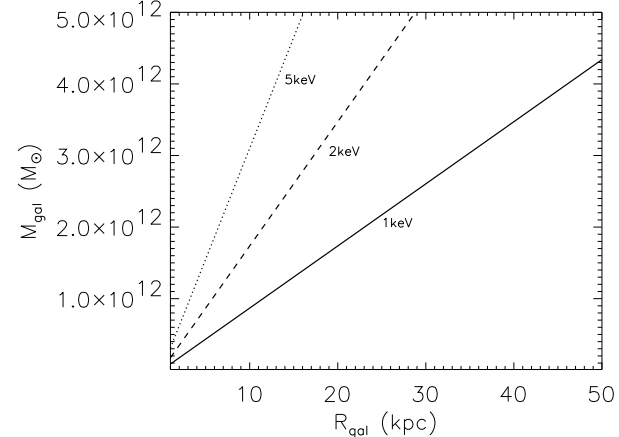


Figure 2. Galaxy mass-radius constraints for B-H accretion in different temperature environments. The lines are for $R_{\text{acc}} = R_{\text{gal}}$ for 1 (solid line), 2 (dashed line), and 5 keV (dotted line) temperature clusters. Equation 12 is only valid for galaxies which lie in the space between the lines and the y -axis.

$$\left(\frac{M_{\text{gal}}}{\text{gr}} \right) \geq 5.6 \times 10^{22} \left(\frac{k T_{\text{ICM}}}{\text{keV}} \right) \left(\frac{R_{\text{gal}}}{\text{cm}} \right) \quad (12)$$

In Fig. 2 we plot the permitted ranges of galactic masses and radii for a range of temperatures of the ICM. Galaxies which lie in the range between the plotted lines and the y -axis will produce large-scale B-H wakes. Figure 2 demonstrates that in high temperature environments, only very compact objects can have galactic wakes produced by the B-H accretion. On the other hand, cool environments are more likely to host galactic wakes.

3.1.2 The velocity of the galaxy

To derive the condition of eq. 12, an average galaxy velocity was assumed, which corresponds to the velocity dispersion σ . In reality, the galaxy velocities are distributed around this value, so that in a cluster there are galaxies which move at lower and larger velocities than σ . The accretion radius of fast moving galaxies becomes very small, and they are not expected to show B-H wakes. It is only the slow moving galaxies which can have large-scale wakes. Comparing eq. 10 and 11, it can be concluded that the subsonic velocity regime is the most prolific condition for B-H wakes.

For the calculations of §2 the ballistic approximation was used. The question that arises is whether such an approximation is valid in the clusters considered. The ballistic approximation assumes that there is no interaction between the deflected particles as they stream past the galaxy on their way to the wake. This assumption is valid only if the kinetic energy of the deflected particles at any distance r from the galaxy is larger than their thermal energy. This condition translates to:

$$v_{\text{gal}}^2 + 2 \frac{GM_{\text{gal}}}{r} \gtrsim \frac{3}{\gamma} c_s^2. \quad (13)$$

Substituting in eq. 13 the distance r by eq. 1 we find that the ballistic approximation is valid only when:

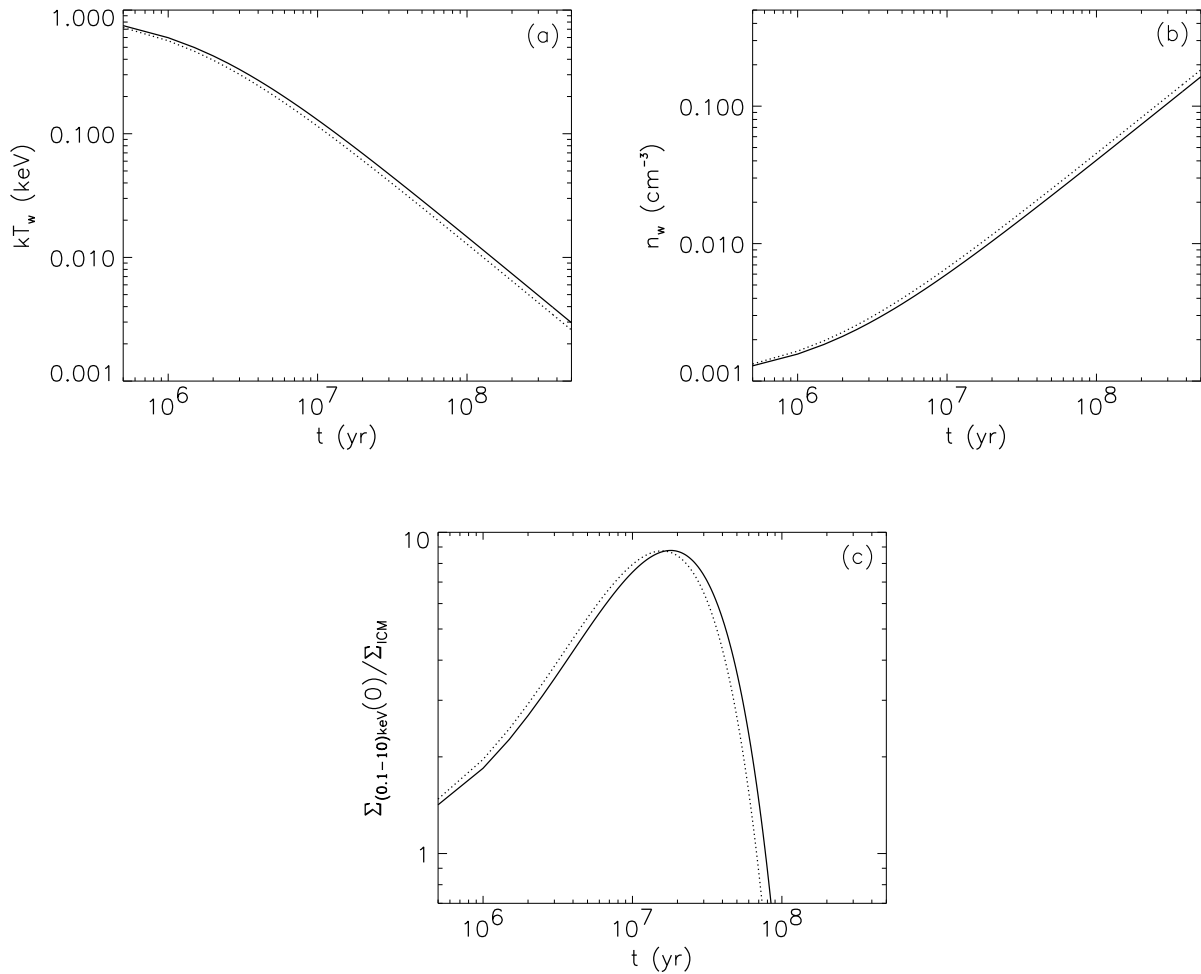


Figure 3. Results of the simulation No. 1 for the two extreme impact parameters (*b*) used in the simulations: 10 kpc (solid line) and R_{acc} (dotted line), which correspond to the closest and furthest parts of the wake to the galaxy (0.5 and 15 kpc respectively along the accretion axis). The evolution of the temperature, number density, and central surface brightness in the energy range (0.1-10) keV are shown in (a), (b), and (c) respectively.

$$v_{\text{gal}}^2 \gtrsim \frac{3 - \gamma}{2\gamma} c_s^2 = 0.4 c_s^2 \quad (14)$$

For any galaxy velocity that obeys eq. 14, the ballistic approximation is correct. Clearly, the lowest limit that eq. 14 defines for v_{gal} is always lower than the average velocity of a cluster galaxy (compare equations 14 and 10).

From the above discussion it is clear that the special conditions of the problem indicate that only slow moving galaxies have wakes with ICM material. We therefore have to restrain the simulations to subsonic regime, which means that virialized cluster galaxies should not show the leading bow-shock, which is a B-H wake's characteristic when the galaxy moves supersonically. We decided to use galaxies velocities equal to the local speed of sound and $0.632 c_s$, as the condition of eq. 14 requires. The additional advantage of the subsonic velocities is that no shock waves are formed as stated above, which would require a different treatment than the one presented here.

4 RESULTS

In the following sections we report on the results of the simulation runs (see Table 1). Figure 3 presents the evolution of the temperature, number density, and central surface brightness of the wake for the simulation No. 1. The results are shown for a distance of 0.5 kpc (solid line) and 15 kpc (dotted line) from the centre of the galaxy along the accretion axis.

4.1 The temperature of the wake

As expected, independently of the environment, the trend in temperature is a continuous cooling with time. The change of the temperature of the wake at a distance of 5 kpc from the galaxy in the three different environments studied is shown in fig. 4.

The signature of the environment is in the rate at which the wake is cooling. In lower temperature clusters the wake cools down more rapidly than in hotter environments: in a

Table 1. B-H accretion : simulations

No	kT_{ICM} (keV)	n_{ICM} ($\times 10^{-3} \text{ cm}^{-3}$)	M_{gal} ($\times 10^{12} M_{\odot}$)	v_{gal} (km s^{-1})	R_{acc} (kpc)
1	1	1	2.5	330	57.3
2	1	1	2.5	516	40.4
3	2	1	2.5	462	28.8
4	2	1	2.5	730	20.2
5	3	1	2.5	565	19.2
6	3	1	2.5	894	13.4

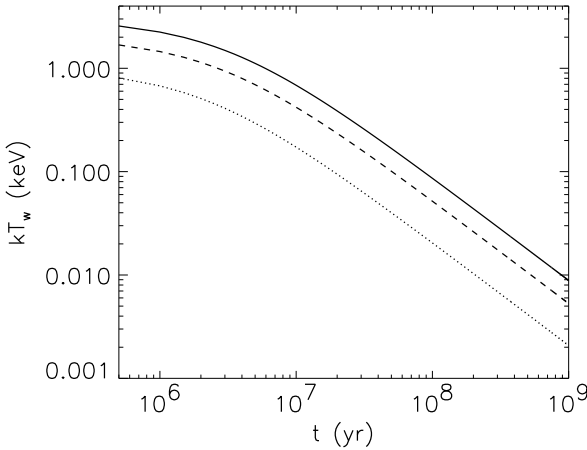


Figure 4. Temperature evolution at a distance of 5 kpc from the galactic centre in different environments: i) $kT_{\text{ICM}}=1 \text{ keV}$ (dotted line), ii) $kT_{\text{ICM}}=2 \text{ keV}$ (dashed line), and iii) $kT_{\text{ICM}}=3 \text{ keV}$ (solid line). In all three cases the galaxy velocity was equal to the local speed of sound.

3 keV cluster, kT_w reaches 10 per cent of the temperature of the surrounding medium in $3 \times 10^7 \text{ yr}$, while a wake in a 1 keV cluster needs approximately half the time to reach the same level. This difference is understood because in low temperature environments, the external pressure is not as large as in hotter clusters: the pressure exerted by the accreted particles (eq. 5) and P_{ICM} are lower in cooler clusters. As a result the overdense wake expands more rapidly, and cools quicker.

The temperature of the wake was also found to depend on the velocity of the galaxy. Figure 5 shows that the lower v_{gal} , the quicker the wake cools. This finding can again be understood in terms of the lower external pressure in cool clusters; the lower v_{gal} is the lower P_{acc} is.

Along the accretion axis we find a decrease in kT_w . At any time, and any environment the temperature at the extremes of the wake is lower than in regions closer to the galaxy (by 10-30 per cent; see fig. 3). Such temperature variations might be measurable with the new x-ray satellites *Chandra* and *XMM-Newton*.

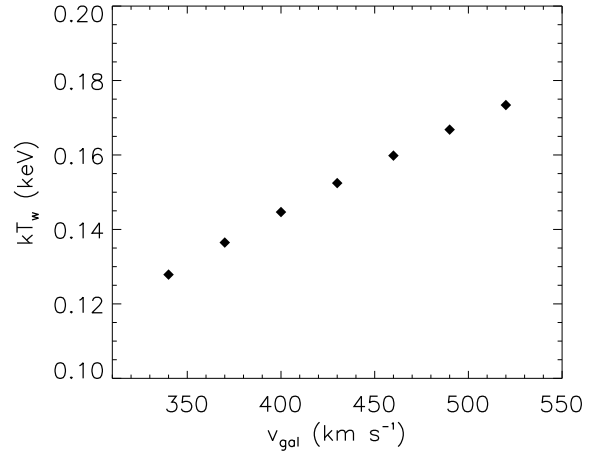


Figure 5. Dependence of the temperature of the wake on the velocity of the galaxy, in a cluster of $kT_{\text{ICM}}=1 \text{ keV}$, and $n_{\text{ICM}} = 1 \times 10^{-3} \text{ cm}^{-3}$. The temperature is measured at a distance of 0.5 kpc from the galactic centre, along the accretion axis, and at a time of $1 \times 10^7 \text{ yr}$.

4.2 The density of the wake

Not surprisingly, the density of the wake increases constantly: in any environment the increase is approximately one order of magnitude in $\sim 10^{7-8} \text{ yr}$. As fig. 6 shows, in higher temperature clusters the density of the wake is lower than in cooler ones. Although the number of ICM particles accreted into the wake per unit time ($d^2 z_{\text{acc}}$) is larger in high kT_{ICM} environments (because the galaxy velocity is larger according to eq. 2), the number density of the wake in poorer environment is larger. This unexpected result can be explained because it is the higher flux of particles ($d^2 z_{\text{acc}}/d\sigma$) that is responsible for the high number density in lower temperature clusters.

Although the effect is not dramatic, in any environment, the wake's number density has its higher value close to the galaxy, and decreases with distance from the galaxy along the accretion axis. This result can be understood in terms of a stronger gravitational potential closer to the galactic centre. Finally, Figure 7 shows the dependence of the wake's number density on the velocity of the galaxy.

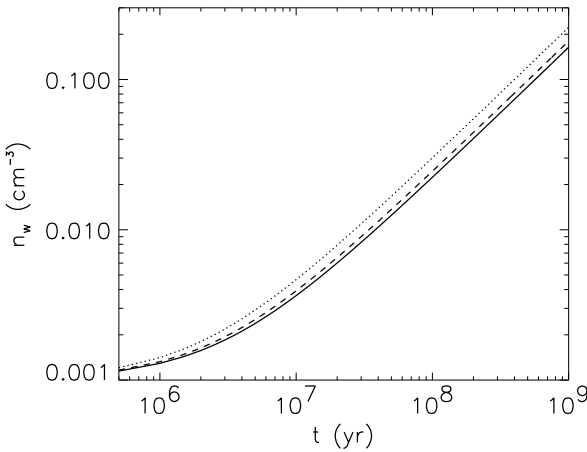


Figure 6. Variations of the number density at a distance of 5 kpc from the galactic centre along the accretion axis. The results for different temperature environments are shown: i) $kT_{\text{ICM}}=1$ keV (dotted line), ii) $kT_{\text{ICM}}=2$ keV (dashed line), and iii) $kT_{\text{ICM}}=3$ keV (solid line). The galaxy velocity was equal to the local sound speed in all three simulations.

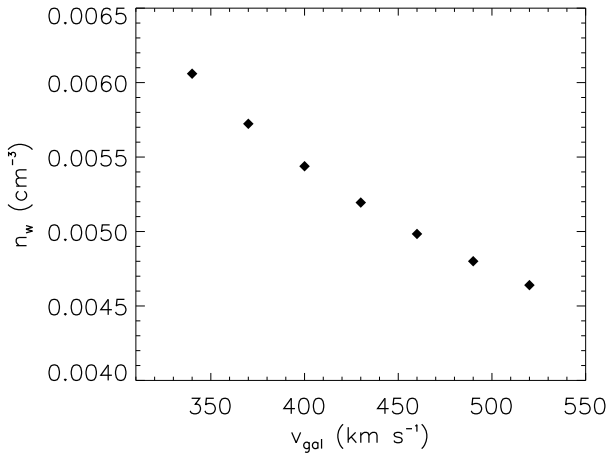


Figure 7. Dependence of the density of the wake on the velocity of the galaxy, in a cluster of $kT_{\text{ICM}}=1$ keV, and $n_{\text{ICM}} = 1 \times 10^{-3} \text{ cm}^{-3}$. The number density is measured at a distance of 0.5 kpc from the galactic centre, along the accretion axis, and at a time of 1×10^7 yr.

4.3 Surface brightness

Figure 8 compares the evolution of the surface brightness $\Sigma_{(0.1-10) \text{ keV}}(0)$ in a 1 keV, 2 keV, and 3 keV clusters. The way that it was calculated is demonstrated in the Appendix A. The conversion to any other energy ranges can be performed by applying eq. A3.

As fig. 8 shows the (0.1-10) keV central surface brightness in any environment increases with time until it reaches 10-30 times the brightness of the surrounding medium. Afterwards, the wake's emission starts declining until it is im-

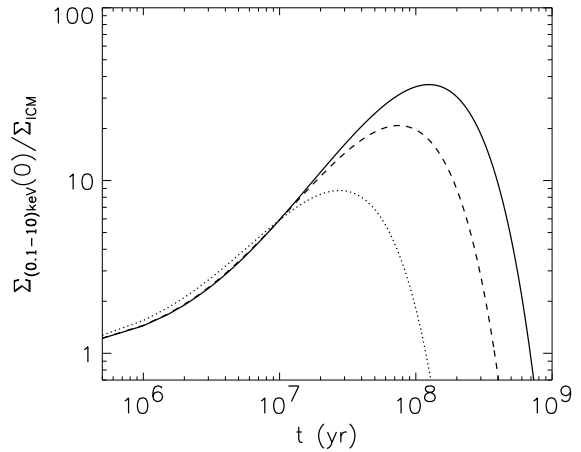


Figure 8. Comparison of the (0.1 - 10) keV central surface brightness in different environments: i) $kT_{\text{ICM}}=1$ keV (dotted line), ii) $kT_{\text{ICM}}=2$ keV (dashed line), and iii) $kT_{\text{ICM}}=3$ keV (solid line). In all cases the galaxy is moving at the local speed of sound (516, 730, and 894 km s⁻¹ respectively), and the profiles presented in this plot correspond to a distance of 5 kpc from the core of the galaxy.

mersed in the background, and the wake becomes undetectable. The time that wakes ‘disappear’ from the x-ray images depends on the richness of the cluster, with higher temperature clusters being able to retain the wake signatures for longer time. Additionally, regions which are further away from the galactic centre fade away quicker than regions closer to the galaxy (fig. 3). The consequence is that a wake becomes shorter with the course of time. As can be inferred from fig. 8, wakes in richer clusters live longer.

4.4 The length of the wake

The maximum length that a wake can reach is simply defined by the ballistic theory as the distance from the galaxy (along the accretion axis) which corresponds to an impact parameter equal to the accretion radius R_{acc} . However, as it was shown earlier, the surface brightness of the wake reaches the background level at times that depend on the richness of the environment. Therefore, it is apparent that the length of the wake depends on the time that it is observed, and the parameters of the environment which they are in. Figure 9 shows for how long the maximum length of a wake is measurable, before the wake is immersed into the background emission. Although wakes in richer environments are shorter, they are detectable for longer periods of time.

5 DISCUSSION

5.1 Comparison with observations

It has been demonstrated that the Bondi-Hoyle accretion alone can give rise to asymmetries in the x-ray images of normal galaxies in relatively rich clusters of galaxies. However, the scale of these asymmetries is small when compared

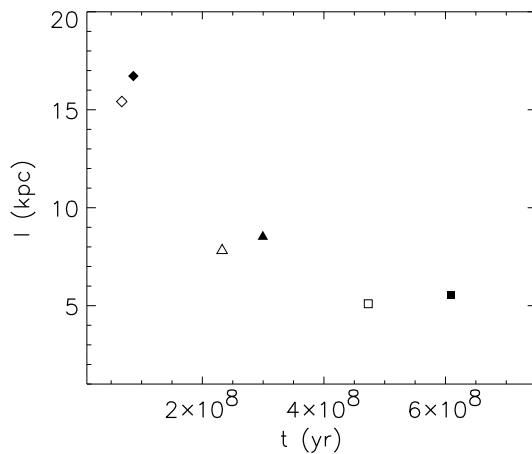


Figure 9. The age of the wake when the surface brightness of the wake's end becomes equal to the surrounding surface brightness versus the maximum length in a 1 keV-cluster (diamonds), 2 keV-cluster (triangles), and 3 keV-cluster (squares). The filled symbols correspond to galaxy velocities equal the local speed of sound (simulations No 2, 4, and 6 respectively). The open symbols are for lower v_{gal} (simulations No 1, 3, and 5).

to the size of the galaxies: in normal conditions the length of a B-H wake cannot exceed ~ 20 kpc. In a cluster at a redshift of $z=0.05$ this length corresponds to ~ 12 arcsec, just above the resolution of the *ROSAT* HRI detector. This fact clearly justifies why wakes have been elusive, and why there are only a few examples reported in the literature. Even with the new x-ray satellites *Chandra* and *XMM-Newton*, wakes will be detectable only in nearby low temperature clusters.

The best known candidate for a B-H wake might be NGC 1404 in the Fornax cluster of galaxies. As seen in the *ROSAT* PSPC image (Jones et al. 1997), its wake points away from NGC 1399, which is the central galaxy in the cluster. In the PSPC data its length appears to be ~ 25 kpc. From Rangarajan et al. (1995) we find that at the distance of NGC 1404 the temperature and number density of the Fornax cluster ICM is $kT_{\text{ICM}} \simeq 1.1$ keV and $n_{\text{ICM}} \simeq 0.6 \times 10^{-3} \text{ cm}^{-3}$. Simulating a galaxy of $M_{\text{gal}} = 2.5 \times 10^{12} M_{\odot}$ moving in an environment defined by the properties of the ICM around NGC 1404, we find that the length of the wake could be ~ 17 kpc if the galaxy is moving on the plane of the sky at a speed of 300 km s^{-1} , and it cannot exceed 20 kpc if the galaxy is moving at 500 km s^{-1} . A first comparison of the PSPC data with the results of the simulation may suggest that B-H accretion cannot create a wake as long as the one observed. However, this inconsistency may indicate that the galaxy is moving at larger speeds than the ones assumed here, owing to recent infall into the cluster. Such speculations cannot be verified, and stringent conclusions cannot be reached before higher spatial and spectral resolution data of NGC 1404 become available, to accurately constrain the parameters of the wake from the x-ray observations.

5.2 Comparison with other simulations

There have been several studies of the B-H accretion since it was first explored by Bondi & Hoyle (1944) in the context of stellar accretion. Hunt (1971) performed quantitative calculations of subsonic and supersonic accretion flows for the case of a point source moving in an adiabatic gas. Sophisticated 3-dimensional simulations have been performed recently (Ruffert 1996 and references there-in). However, most of these simulations were not designed to represent the conditions encountered in clusters of galaxies. They explored either temperature and density regimes which were not representative of clusters of galaxies, or the galaxy velocities used were too high. Additionally, the results of these studies cannot be easily converted to observables, making a comparison with x-ray observations not straightforward. However, these simulations provide a first picture of the results presented here. The simulations of a galaxy moving subsonically presented by Ruffert (1994) show that a downstream over-density is created. The offset from the centre of the accretor is small compared to the supersonic examples. Additionally, as it is clear from the results of Ruffert (1994), in the supersonic case there is no bow-shock in front of the galaxy. On the other hand the bow-shock is the most prominent structure generated by the B-H accretion onto a supersonically moving body. As stated by Ruffert (1994), a B-H wake in the subconic case “*is the result of the superposition of the slow radial flow into the accretor and the relative motion between the accretor and the medium*”.

Recently, more in depth predictions of the ICM/ISM interactions in clusters of galaxies have been presented by Stevens et al. (1999). Their simulations allow both dynamical processes to take place: ICM is deflected and concentrated behind the moving galaxy, and ram pressure strips the galactic ISM. The result is the creation of downstream density enhancements, which consist of both galactic and intracluster material. Unfortunately, this study does not assess the fraction of each component expected in the wake for a variety of environmental conditions. As a result, one cannot confidently estimate whether the wakes we observe consist of galactic or ICM material.

However, these simulations give the first indication that B-H accretion might dominate in low temperature clusters, in agreement with our results, and ram pressure creates wakes in richer clusters. If one was to compare the results of the present study with the simulations of Stevens et al., he would have chosen to use their simulation No. 1b, for the sake of consistency. Indeed, simulation No. 1b presents the results of a galaxy/ICM interaction in a cluster with temperature $kT_{\text{ICM}}=1$ keV, and density $n_{\text{ICM}} \sim 4 \times 10^{-4} \text{ cm}^{-3}$. These parameters of the ICM correspond well to the conditions studied here. Generally, there is a good agreement between both studies: they both predict an increase of approximately two orders of magnitude in the n_w , with a simultaneous temperature drop by two orders of magnitude at 5 kpc along the accretion axis and after 5×10^8 yr (see fig. 3 in Stevens et al.). The agreement between the two studies may lead to the false conclusion that both simulations describe the same physical process successfully. However, special care must be paid, because the galaxy velocity in Stevens et al. is supersonic with $v_{\text{gal}} = 960 \text{ km s}^{-1}$. As it was proven in the previous sections, such velocity regimes cannot produce

large-scale B-H wakes, because the accretion radius is too small. However, the lack of striking differences make us conclude that B-H dominates in No. 1b simulation of Stevens et al.

6 SUMMARY AND CONCLUSIONS

The motion of a body through a gaseous medium results in the creation of an overdense, cool wake: the gravitational attraction of the body deflects the surrounding medium's particles, which end up being concentrated behind it. This process (Bondi-Hoyle accretion) was first explored by Bondi & Hoyle (1944) in the context of stellar accretion. The aim of this paper was to investigate if this process is at work in clusters of galaxies, which clusters are the best hosts of B-H wakes, and if such features can be seen in the x-ray data of clusters of galaxies.

The main results of our calculations can be summarized as follows:

- In clusters of galaxies, the ICM can be concentrated behind the subsonically moving galaxies, although the results of B-H accretion are expected to be more dramatic when the galaxies move supersonically.
- Large-scale B-H wakes can be found only in low temperature clusters, behind slow moving, and massive galaxies.
- A stable situation is not reached within reasonable timescales: the wake is created, its temperature decreases and its density increases constantly.
- The smaller the temperature of the ICM, the longer the wake is. However, wakes in richer clusters live longer and are brighter. Such features will be easily detectable with the *Chandra* and *XMM-Newton* satellites in nearby, poor clusters of galaxies.
- The central, x-ray surface brightness of the wake can reach 10-30 times the brightness of the surrounding medium.
- The properties of a B-H wake depend on the velocity of the galaxy. Fast moving galaxies, for example, have hotter wakes. On the other hand, galaxies with pronounced B-H wakes should not have bow shocks, because their motion is subsonic.

ACKNOWLEDGMENTS

We would like to thank M. Cropper for useful discussion, and J. Lee for critical reading of the manuscript. Special thanks to C. Lee for the encouragement to undertake this investigation.

REFERENCES

Bondi H., 1952, MNRAS, 112, 195
 Bondi H., Hoyle F., 1944, MNRAS, 104, 273
 Hunt R., 1971, MNRAS, 154, 141
 Jones C., Stern C., Forman W., Breen J., David L., Tucker W., Franx M., 1997, ApJ, 482, 143
 Rangarajan F.V.N., White D.A., Ebeling H., Fabian A.C., 1995, MNRAS, 277, 1047
 Ruffert M., A&AS, 106, 505
 Ruffert M., 1996, A&A, 311, 817

Stevens I.R., Acreman D.M., Ponman T.J., 1999, MNRAS, 310, 663
 White D. A., Jones C., Forman W., 1997, MNRAS, 292, 419
 Wu X.-P., Fang L.-Z., Xu W., 1998, A&A, 338, 813

APPENDIX A: BOLOMETRIC LUMINOSITY AND SURFACE BRIGHTNESS DISTRIBUTION

The bolometric luminosity $L_{\text{bol}}(x, t)$ used in eq. 7 to describe the energy radiated away, is found by integrating the bremsstrahlung emissivity over the volume of the wake (V_w) at any time t :

$$L_{\text{bol}}(x, t) = 6.8 \times 10^{-38} \frac{k^{1/2}}{h} \bar{g}_B \int k T_w^{1/2}(x, t) n_w(x, t)^2 dV_w \quad (A1)$$

If we assume that the emitting region is a cylinder, the gas in the wake is uniformly distributed, and it emits isotropically, the surface brightness $[\Sigma_{E_1-E_2}(\theta)]$ at any distance θ from the accretion axis is the integrated bremsstrahlung emissivity along a column at the projected distance θ from the accretion axis:

$$\Sigma_{E_1-E_2}(\theta) = 6.8 \times 10^{-38} n_w^2 T_w^{-1/2} \bar{g}_B I_{E_1-E_2} \int_{r=\theta}^{r=R_w(x, t)} \frac{r dr}{\sqrt{r^2 - \theta^2}} \quad (A2)$$

where $I_{E_1-E_2}$ the integral which defines the energy range in which $\Sigma_{E_1-E_2}(\theta)$ is calculated, and it is given by:

$$I_{E_1-E_2} = \int_{\nu_1}^{\nu_2} \exp\left(-\frac{h\nu}{kT_w}\right) d\nu \quad (A3)$$

Integrating eq. A2 we find that the surface brightness at any point θ is:

$$\Sigma_{E_1-E_2}(\theta) = \Sigma_{E_1-E_2}(0) \left[1 - \left(\frac{\theta}{R_w(x, t)} \right)^2 \right]^{1/2} \quad (A4)$$

where the central surface brightness $\Sigma_{E_1-E_2}(0)$ is given by:

$$\Sigma_{E_1-E_2}(0) = 13.6 \times 10^{-38} n_w^2 T_w^{-1/2} \bar{g}_B I_{E_1-E_2} R_w(x, t) \quad (A5)$$